A Parametric Investigation of PBI and AASF Scalarizations

Hemant Kumar Singh
University of New South Wales
Canberra, ACT 2600, Australia
h.singh@adfa.edu.au

Kalyanmoy Deb
Michigan State University
East Lansing, MI 48823, USA
kdeb@egr.msu.edu

ABSTRACT

Multi-objective problems (MOP) are of significant interest to both multi-criteria decision making (MCDM) and evolutionary multi-objective (EMO) research communities. A core technique common in both is *scalarization*, which combines multiple objectives into one in a way that solving it provides a solution to the original MOP. In this paper, we look closely at two scalarization methods – augmented achievement scalarization function (AASF) and penalty boundary intersection (PBI). While the former has its roots in MCDM literature, the latter was developed in EMO field with focus on decomposition-based algorithms. We observe the conventional limits of the parameters involved in these methods and then demonstrate that by relaxing those limits one could be made to behave like the other. The aim is to gain a deeper understanding of both these measures, as well as expand their parametric range to provide more control over the search behavior of EMO algorithms. It also lays groundwork for further development of complete analytical derivations of equivalence conditions between the two metrics.

CCS CONCEPTS

• **Applied computing** → **Multi-criterion optimization and decision-making**;

ACM Reference Format:
Hemant Kumar Singh and Kalyanmoy Deb. 2019. A Parametric Investigation of PBI and AASF Scalarizations. In *Proceedings of the Genetic and Evolutionary Computation Conference 2019 (GECCO '19 Companion)*. ACM, New York, NY, USA, 2 pages. https://doi.org/10.1145/3319619.3321886

1 INTRODUCTION AND BACKGROUND

Scalarization is commonly used in contemporary EMO algorithms for approximating the Pareto front using decomposition-based methods, and in MCDM for arriving at a solution suitable to a decision-maker. In this study, we attempt to establish the commonalities in behavior between two oft-used scalarizing measures - AASF [3] originating from MCDM literature and PBI [4] originating from EMO literature. Such parallels have not been observed in literature so far due to a restricted range in which the parameters of these two metrics are used, the reasons for which lie in their conception. For example, PBI uses a parameter θ to impose a *penalty* term, and therefore is always assumed to be greater than 0 (often set to 5). AASF uses a parameter ρ which attempts to change the ASF contours *slightly* in order to avoid weakly non-dominated solutions; and hence it is usually restricted to a very small positive value close to 0 (e.g. 10^{-4}). Although some studies have investigated their parametric behavior individually (e.g. [2]), to the authors' knowledge, the relations between them have not been studied previously.

To calculate AASF and PBI for a given candidate solution $P = (p_1, p_2)$ in the objective space, a reference point $Z = (z_1, z_2)$ and a reference vector $\mathbf{w} = (w_1, w_2)$ are required, such that $w_1 + w_2 = 1$. Z is often chosen as the *ideal* point formed by they coordinates of best objective values along each axis. Since the two objectives can be in different orders of magnitude, it is a common practice to linearly normalize the objective space between [0,1] before conducting any distance based calculations, which maps Z to (0,0). With reference to Fig. 1(a)-(b), AASF and PBI can be calculated as shown in Eq. 1. The corresponding contours can be visualized in Fig. 1(c)-(d).

$$\begin{aligned} &AASF(\mathbf{f}, \mathbf{w}, \mathbf{z}, \rho) = \max_{i=1}^{M}\left(\frac{f_i}{w_i}\right) + \rho\sum_{i=1}^{M}\left(\frac{f_i}{w_i}\right) \quad \text{if } z_i = 0\forall i; \\ &PBI(\mathbf{f}, \mathbf{w}, \mathbf{z}, \theta) = d_1 + \theta d_2; d_2 = \frac{|w_1 f_2 - w_2 f_1|}{\sqrt{w_1^2 + w_2^2}}, d_1 = \sqrt{|P|^2 - d_2^2} \end{aligned} \tag{1}$$

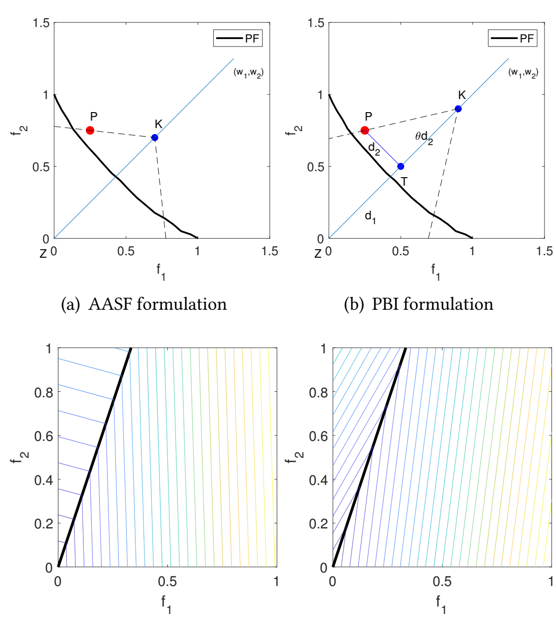

(a) AASF formulation

(b) PBI formulation

(c) AASF contours, $\rho = 0.1$

(d) PBI contours, $\theta = 5$

Figure 1: Formulation and contours of AASF and PBI

GECCO '19 Companion, July 13–17, 2019, Prague, Czech Republic

ACM ISBN 978-1-4503-6748-6/19/07…$15.00
https://doi.org/10.1145/3319619.3321886

2 PARAMETRIC STUDY

Let us start by considering the conventional bounds of the two parameters *in their entirety*, i.e., $\theta \in [0, \infty)$ and $\rho \in [0, \infty)$ instead of only the specific values used in literature. We consider an off-center reference vector (RV), $\mathbf{w} = (0.25, 0.75)$, so that the asymmetric nature of AASF could be accounted for. We refer to the angle made by the isolines to the RV as ϕ for PBI. For AASF, the contours are asymmetric about the RV, so we refer to the angle above and below the RV with respective contour lines ϕ_a and ϕ_b respectively. These variations are shown in Fig. 2. It can be noted that for PBI, $\phi \in (0, 90^\circ]$, whereas for AASF, $\phi_a \in [71.6^\circ, 143^\circ)$ and $\phi_b \in [18.4^\circ, 36.9^\circ)$.

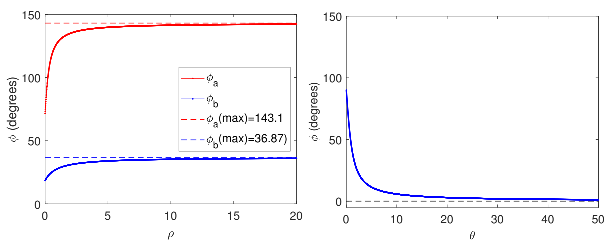

(a) AASF (b) PBI

Figure 2: (a) Variation of ϕ_a, ϕ_b with ρ for $\mathbf{w} = (0.25, 0.75)$ for AASF; (b) Variation of ϕ with θ (regardless of w) for PBI

Thus, there exists a range of angles that that could be achieved by PBI *but not* AASF, i.e. $(0, 18.4^\circ)$, and also a range which could be achieved by AASF *but not* PBI, i.e., $\phi_a \in (90^\circ, 143^\circ)$, for *any* $\rho, \theta \in [0, \infty)$. Therefore, in order to make these two metrics behave identically, the parameters θ and ρ need to be relaxed beyond their originally conceived bounds. In Fig. 2(a), it can be seen that if ρ axis of AASF is allowed to extend below 0, angles of up to $\phi_a, \phi_b = 0$ will be achievable (as the graph is strictly increasing) to match the PBI. Both ϕ_a and ϕ_b go to 0 at $\rho = -1/2$. Similarly, if θ axis of PBI is allowed to extend below 0 (Fig. 2(b)), a higher value of ϕ can be achieved (as the graph is strictly decreasing) to match AASF behavior. The variations with the extended ranges are shown in Fig 3. This now makes it possible to consider any value of ρ in Fig 3(a) and find the corresponding ϕ_a, ϕ_b. Subsequently, the corresponding values of θ_a and θ_b can be determined from Fig 3(b) and used to calculate an equivalent PBI function that matches the AASF function contours for the given ρ.

3 PROOF OF PRINCIPLE RESULTS

In order to verify the above way of finding equivalent PBI parameters (θ_a, θ_b) for a given AASF parameter ρ, we use the Non-dominated Sorting Genetic Algorithm III (NSGA-III) [1] framework. In NSGA-III, the survival in the last non-dominated front (that can not be contained within the population size N) is done through niche preservation operation using reference vectors. The solutions assigned to any given niche are ranked based on the their closest perpendicular distance (d_2) to the associated reference direction, and the one with the least d_2 is considered the selected point for that direction. Using this ranking process, the required number of surviving solutions are selected. To demonstrate the idea discussed

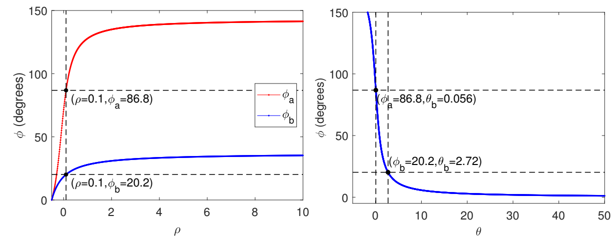

(a) AASF (b) PBI

Figure 3: (a) Variation of ϕ for PBI (b) Variation of ϕ_a, ϕ_b for $\mathbf{w} = (0.25, 0.75)$ for AASF.

above, two simple variants are created: (a) NSGAIII-AASF, where d_2 is replaced by AASF (with a given ρ), and (b) NSGAIII-EPBI, where an 'equivalent' PBI is used with the corresponding θ values calculated for each reference vector to match the prescribed $\rho = 0.1$. Proof of principle results are presented on two ZDT problems [5] in Fig. 4, where the same final population is obtained using the above two variants. The behavior is consistent across multiple instantiations. The above parametric study and preliminary results confirm in principle that it is possible to find settings for which the two scalarization methods, AASF and PBI, would exhibit the same type of search behavior. The future work will delve into these transformations analytically and investigating their utilization for controlling the search using their entire parametric range.

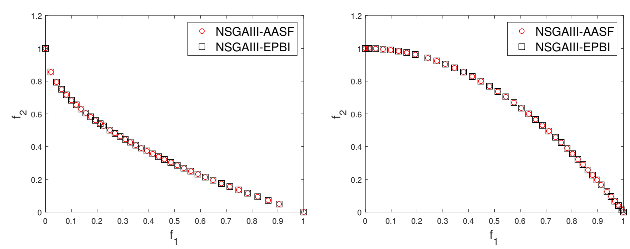

(a) ZDT1 (b) ZDT2

Figure 4: Final populations: $\text{NSGAIII}_{\text{AASF}}$ and $\text{NSGAIII}_{\text{EPBI}}$

REFERENCES

[1] Kalyanmoy Deb and Himanshu Jain. 2014. An Evolutionary many-objective optimization algorithm using reference-point based non-dominated sorting approach, Part I: solving problems with box constraints. *IEEE Transactions on Evolutionary Computation* 18, 4 (2014), 577–601.

[2] Hisao Ishibuchi, Naoya Akedo, and Yusuke Nojima. 2013. A study on the specification of a scalarizing function in MOEA/D for many-objective knapsack problems. In *International Conference on Learning and Intelligent Optimization*. Springer, 231–246.

[3] Kaisa Miettinen. 2012. *Nonlinear multiobjective optimization*. Vol. 12. Springer Science & Business Media.

[4] Qingfu Zhang and Hui Li. 2007. MOEA/D: A multi-objective evolutionary algorithm based on decomposition. *IEEE Transactions on Evolutionary Computation* 11, 6 (2007), 712–731.

[5] Eckart Zitzler, Kalyanmoy Deb, and Lothar Thiele. 2000. Comparison of multiobjective evolutionary algorithms: Empirical results. *Evolutionary computation* 8, 2 (2000), 173–195.